




Neutrophil extracellular traps (NETs) infiltrate haematoma and surrounding brain tissue after intracerebral haemorrhage: A post-mortem study

Laurent Puy¹  | Delphine Corseaux² | Romain Perbet^{1,3} | Vincent Deramecourt^{1,3} | Charlotte Cordonnier¹  | Vincent Bérézowski¹ 

¹U1172-LiNCog-Lille Neuroscience & Cognition, Univ. Lille, Inserm, CHU Lille, Lille, France

²Inserm, CHU Lille, Institut Pasteur de Lille, U1011-EGID, Univ. Lille, Lille, France

³Institute of Pathology, Centre de Biologie Pathologie, Lille University Hospital, Lille, France

Correspondence

Charlotte Cordonnier, Univ. Lille, Inserm, CHU Lille, U1172-LiNCog-Lille Neuroscience & Cognition, F-59000 Lille, France.
Email: charlotte.cordonnier@univ-lille.fr

Funding information

This work was supported by the Fondation Recherche sur les Accidents Vasculaires Cérébraux (project FRAVC180713012), the Fondation pour la Recherche Médicale (FDM201806006375, fellowship L.P.) and the Fondation I-SITE ULNE (fellowship L.P.).

[Correction added on 16 June 2021, after first online publication date: The article title was previously incorrect and has been updated in this current version.]

Abstract

Aims: Because of their prothrombotic and neuroinflammatory effects, neutrophils and neutrophil extracellular traps (NETs) represent interesting therapeutic targets for spontaneous intracerebral haemorrhage (sICH). We investigated the presence, spatial and temporal distribution of NETs in a human sICH post-mortem study.

Methods: From 2005 to 2019, all sICH patients who came to autopsy within the first month after stroke were included and grouped according to the timing of death: 72 h, 4–7 days, 8–15 days and >15 days after ICH onset. Paraffin-embedded tissue was extracted from four strategic areas: haematoma, peri-haematoma area, ipsilateral surrounding brain tissue and a control contralateral area. Myeloperoxidase and histone H3 citrulline were immunolabelled to detect neutrophils and NETs respectively.

Results: Neutrophils were present in the brains of the 14 cases (4 men, median age: 78 years) and NETs were found in 7/14 cases. Both neutrophils and NETs were detected within the haematoma but also in the surrounding tissue. The appearance of neutrophils and NETs was time-dependent, following a two-wave pattern: during the first 72 h and between 8 and 15 days after ICH onset. Qualitative examination showed that neutrophils and NETs were mainly located around dense fibrin fibres within the haematoma.

Conclusions: These observations provide evidence for NETs infiltration in the brain of patients who die from sICH. NETs might interact with early haemostasis within the haematoma core, and with the surrounding neuroinflammatory response. These findings open research perspectives for NETs in the treatment of sICH injuries.

KEYWORDS

Stroke, intracerebral haemorrhage, post-mortem, neutrophils, neutrophil extracellular traps

INTRODUCTION

Spontaneous intracerebral haemorrhage (sICH) is the most feared cerebrovascular event because it is associated with a high rate of mortality and morbidity, and devoid of specific treatment.¹ Unfortunately to date, interventions to enhance haematoma clearance using recombinant tissue-plasminogen activator (rtPA) infusion

have failed, as well as promising experimental neuroprotective treatments to reduce secondary brain tissue damage.^{2,3}

Following the rapid accumulation of blood within the brain parenchyma, neutrophils are the first inflammatory cells to reach the haematoma site.^{4,5} In addition to the well-established neurotoxicity attributed to their prolonged activation,^{4–7} extensive data from ischaemic stroke studies demonstrate a direct action of neutrophils

on clot resistance to rtPA.⁷ Furthermore, neutrophils are able to cast out nuclear DNA/histone meshworks, named neutrophil extracellular traps (NETs). The so-called NETosis is a regulated process of neutrophil cell death that contributes to the host defence against various pathogens. NETs correspond to extracellular web-like structures composed of nuclear and/or mitochondrial DNA (decondensed chromatin) and granular contents. Their histopathological identification is based on positive staining for citrullinated histone 3, because histones are the most abundant protein components of NETs.

Upon induction of NETosis, oxidative stress leads to the production of hydrogen peroxide through the NADPH oxidase complex. Hydrogen peroxide is a substrate of myeloperoxidase (MPO) and induces the release of neutrophil elastase (NE) from neutrophil granules. NE subsequently migrates to the nucleus to induce histone degradation, which in turn, leads to DNA decondensation. When the nuclear membrane disintegrates, the decondensed chromatin mixes with cytosolic and granular proteins and the whole complex is then expelled from the neutrophil to form NETs.^{8,9}

Data on NETs in the setting of cerebrovascular diseases mainly come from the ischaemic stroke literature: NETosis has been shown to promote resistance to rtPA in the intravascular thrombus¹⁰ and may have an inflammatory-mediated deleterious effect on the brain parenchyma.¹¹

As sICH also comprises a neuroinflammatory phase, we hypothesised that NETs might have a key role in the pathophysiology of sICH. Recent experimental data suggested that NETs impaired the efficacy of rtPA-mediated fibrinolysis of the ICH clot in rats.¹² The translation of these data into therapeutic strategies requires the presence of NETs to be demonstrated in human brain tissue after sICH, in relation to the temporal pattern of neutrophil infiltration.

We investigated the histopathologic presence of NETs and describe their spatial and temporal distribution in the core of the haematoma and surrounding brain tissue of sICH patients.

METHODS

Human brain sampling

We included all consecutive cases (2005–2019) from the Lille University Hospital brain bank (Lille Neurobank, France) of sICH patients who came to autopsy within the first month after the onset of a stroke.¹³ Patients had been admitted to the Lille University Hospital. Autopsies were performed within 12–36 h after death, and hemispheres were fixed in formalin for 4 to 8 weeks. Data regarding location and dimension of the haematoma were extracted from the standardised post-mortem reports. sICH volume and volume of cerebral oedema were manually segmented using Mango[®] software from the in-hospital imaging database. The brain sampling comprised relatively large sections (average size 6.5 cm). To assess the potential spreading of neutrophils and NETs within ICH core and surrounding tissue, paraffin-embedded tissue blocks were analysed from four distinct areas (Figure 1): (1) within the haematoma (2–4 blocks per case), (2) within the peri-haematoma area (PHA, 2–4 blocks per case), (3) next to the PHA within ipsilateral surrounding brain tissue (ISBT) (2–3 blocks per case). ISBT was defined as the area adjacent to the PHA where the tissue exhibited normal integrity. Lastly, a fourth control area was analysed (i.e. frontal and/or occipital lobes from the contralateral hemisphere in most of the cases). All post-mortem examinations and neuropathologic diagnosis of the underlying cause of sICH were performed by an experienced neuropathologist (V.D).

Standard protocol approvals, registration and patient consents

Human brains were obtained from the Lille Neurobank (CRB/CIC1403 Biobank, BB-0033-00030, agreement DC-2008-642), which fulfils the criteria of the local laws and regulations on biological

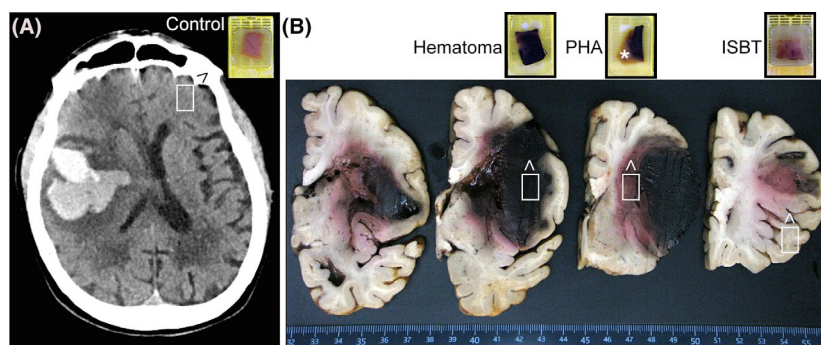


FIGURE 1 Study design. (A) CT scan of a representative patient performed 14 days after symptom onset. Hyperdense lobar intracerebral haemorrhage is shown, surrounded by hypodense peri-haematoma oedema. (B) Formalin-fixed hemispheres of spontaneous intracerebral haemorrhage (sICH) cases were cut into 5-mm-thick blocks taken from 4 specific areas: haematoma, peri-haematoma area (PHA), ipsilateral surrounding brain tissue (ISBT) and contralateral block as reference. Four adjacent 5 µm-thick sections were cut from these blocks and stained with haematoxylin & eosin, Martius Scarlet Blue, and immunolabelled for myeloperoxidase and histone H3 citrulline to detect neutrophil extracellular traps (NETs)

resources with donor consent, data protection and ethical committee review.

Staining and immunohistochemistry

Sections of formalin-fixed paraffin-embedded tissue were stained with haematoxylin–eosin (H&E) for a global identification and structural analysis of the tissues. Martius Scarlet Blue (MSB) staining was then used to identify fibrin (dark pink to red), red blood cells (orange to yellow) and collagen of the vessel wall (blue) to better characterise the areas of bleeding. The MSB staining protocol was as follows: sections were immersed in Bouin's fluid (HT-10132; Sigma-Aldrich) at 60°C for 1 h, after which the sections were washed three times in distilled water and placed in an Autostainer (Leica) for the staining procedure. Sections were immersed in 95% ethanol for 5 min. Sections were then immersed in Naphthol Yellow S (sc215544; Santa Cruz Biotechnology, Heidelberg, Germany) for 2 min followed by five washing steps of 1 min each in distilled water. Subsequently, sections were immersed in Crystal Ponceau 6R (sc214779; Santa Cruz Biotechnology) for 10 min and differentiated in 1% phosphotungstic acid (79690, Sigma-Aldrich) for 10 min to remove all non-specific Crystal Ponceau staining. Finally, sections were immersed in Methyl Blue (M5528; Sigma-Aldrich) for 5 min at room temperature, followed by a washing step in 1% acetic acid and a rapid dehydration by transferring the sections in solutions of increasing ethanol concentration, until 100% ethanol was reached. Next, sections were immersed in a xylene-derivative Sub-X and mounted using Sub-X mounting medium (3801740, Leica).

Myeloperoxidase (MPO) was immunolabelled to identify neutrophils, using a VENTANA BenchMark GX immunohistochemistry automated staining machine (Roche). The primary antibody was a rabbit polyclonal IgG (Ventana-Roche). We used the i-View DAB detection kit[®] (Ventana Medicals System, Roche Group) as an indirect biotin streptavidin system for the detection of the primary IgG antibody. Tissue sections were counterstained using bluing reagent solution (Ventana-Roche). The presence of NETs was assessed by a rabbit polyclonal primary antibody to histone H3 citrulline (ref ab5103, 0.3 µg/ml, and nucleated cells were stained green using a Methyl Green solution (H-3402, Vector Laboratories). For each immunostain, a tissue section was processed identically except that the primary antibody was omitted as a specificity control and revealed no signal (data not shown). MSB staining, as well as MPO and histone H3 citrulline immunolabelling were performed on serial-sections of 5 µm each. A bright-field slide scanner (Zeiss Axioscan Z1) digitised the whole tissue section at 20-fold magnification after staining. Immunolabelled sections were independently analysed by two experienced operators (L.P. and V.B). A staining surface ratio ([stacking surface/whole section surface]*10³) was calculated with a semi-automated method using ImageJ software in order to quantify the positively stained or labelled surface in each area (i.e. haematoma core, PHA and ISBT).

Statistical analysis

Continuous, ordinal and categorical variables were expressed as the mean ± SD, the median [interquartile range] or the number (percentage) respectively. A first analysis aimed at comparing areas of interest (that encompass haematoma, PHA and ISBT) and the control block from the contralateral hemisphere. To do so, bivariate comparisons were performed using Student's *t* test or Mann–Whitney *U* test as appropriate. To assess the temporal changes, sICH cases were grouped according to the time of death: 72 h (*n* = 2), 4–7 days (*n* = 4), 8–15 days (*n* = 5) and >15 days (*n* = 3). We used a Kruskal–Wallis with Tukey *post hoc* tests to compare the different timepoints within the areas of interest. GraphPad Prism software was used to perform the statistical analysis, with the *p*-value considered as significant when < 0.05.

RESULTS

Study population

Between 2005 and 2019, 22 patients with sICH came to autopsy. Among them, three sICH were due to an underlying vascular malformation (arteriovenous malformation, *n* = 2 and cavernous malformation, *n* = 1) and five patients had died more than 1 month after sICH onset. Therefore, we included 14 sICH cases in the present study (median age: 78 [76–85] years, 4 males / 10 females). Median sICH and oedema volumes were 90 [61–112] cm³ and 74 [68–94] cm³ respectively. Characteristics of each case are reported in Table 1.

Neutrophils: presence, spatial distribution and temporal pattern

Neutrophils were observed in all cases (*n* = 14/14). All ipsilateral formalin-fixed paraffin-embedded sections had increased neutrophil counts compared to control contralateral sections in which no neutrophils were observed within the tissue (*p* < 0.0001). Neutrophil distribution followed a centripetal gradient from the ipsilateral surrounding brain tissue to the haematoma core (0.16 [0.11–0.41] for the ipsilateral surrounding brain tissue; 14.67 [2.4–19.3] for the PHA and 41.5 [11.2–94.9] for the haematoma core, *p* < 0.0001). Kinetic evolution of neutrophil immunolabelling in each area of interest is reported in Figure 2. Neutrophils labelling varied over time in each area of interest (Kruskal–Wallis test: *p* = 0.042, 0.038 and 0.034 for haematoma, PHA and ISBT respectively), as detailed below:

Neutrophils within the haematoma

Neutrophils (Figure 2B) were observed within the haematoma as early as the first 24 h (staining surface ratio: 72.14 [62–82]). The MPO-labelled surface decreased by 80% between day 4 and day 7

TABLE 1 Characteristics of the study population

Number	Age	Sex	Past history of Hypertension	Antithrombotic use at the time of ICH onset	ICH location	sICH aetiology ^a	ICH volume (cm ³)	Oedema volume (cm ³)	Time from ICH to death (days)
1	84	F	no	yes	Lobar	CAA	113	67	1
2	65	F	no	yes	Lobar	CAA	114	74	2
3	84	F	yes	no	Lobar	CAA	87	105	4
4	76	F	no	yes	Lobar	CAA	82	93	5
5	89	F	no	no	Lobar	CAA	93	102	5
6	86	F	yes	yes	Lobar	CAA	-	-	6
7	89	F	yes	no	Lobar	CAA	53	69	8
8	76	M	yes	no	Deep	HTN-SVD	46	63	8
9	78	F	yes	yes	Lobar	CAA	63	74	10
10	76	F	no	no	Lobar	CAA	42	47	13
11	73	M	yes	no	Lobar	CAA	163	68	14
12	85	M	yes	no	Lobar	CAA	107	96	17
13	78	M	yes	no	Lobar	CAA	-	-	27
14	71	F	no	no	Lobar	CAA	111	78	30

Note: CAA: Neuropathologic diagnosis was confirmed by Red Congo staining and Amyloid β 40 immunolabelling by one experienced neuropathologist (V.D). The first evidence for NETs infiltration following intracerebral haemorrhage in the human brain.

Abbreviations: CAA, cerebral amyloid angiopathy; F, female; HTN- SVD, hypertensive small vessel diseaseM, male; PHA, peri-haematoma area; sICH, spontaneous intracerebral haemorrhage.

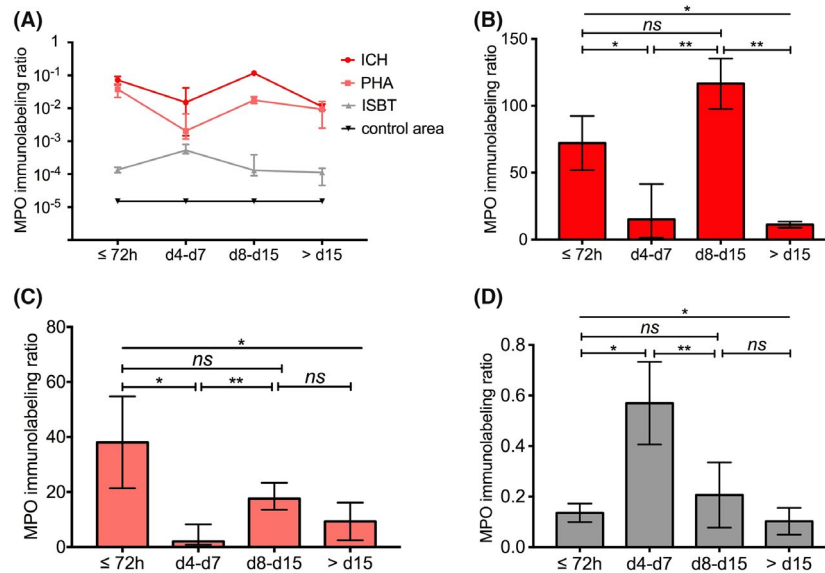


FIGURE 2 Temporal and spatial distribution of neutrophils in the human brain after intracerebral haemorrhage. (A) Immunolabelling ratio ([stacking surface/whole section surface] $\times 10^{-3}$) of neutrophil myeloperoxidase (MPO) in the post-mortem brain tissue of 14 patients deceased from spontaneous intracerebral haemorrhage at different time periods after onset (before 72 h, from day 4 to day 7, from day 8 to day 15, above day 15). Curves refer to the ratios calculated in brain areas of interest including the haematoma (ICH), the peri-haematoma area (PHA), the ipsilateral surrounding brain tissue (ISBT), and the contralateral area (control area). Bars and symbols correspond to the median value and the width of the 95% CI. Data were log10-transformed for an easier comparison between ICH, PHA, ISBT and control areas. Raw ratios are presented in histograms for ICH (B), PHA (C) and ISBT (D) areas for statistical analysis. Ratios were significantly different between time points according to Kruskal-Wallis followed by a Tukey *post hoc* test (** $p \leq 0.01$, * $p \leq 0.05$; ns: not significant)

(15.12 [2.3–31], $p = 0.048$). In brains of patients who died between day 8 and day 15 after sICH, we observed a 7.8-fold increase in MPO expression (116.66 [107–126], $p = 0.001$). In the brains of patients who died after day 15, the MPO-labelled surface drastically decreased by 90% (11.18 [10–12], $p = 0.005$). Interestingly, qualitative examination revealed that neutrophils deposited preferentially close to dense fibrin fibres (Figure 3D,E). Spatial distribution of neutrophils within the haematoma also varied over time; within the first 72 h neutrophils were more frequently observed in the periphery (75.40% of immunolabelled surface) than in the core of the haematoma (24.6%). Between day 4 and day 7, the opposite situation was observed, 76.8% in the core vs 23.2% in the periphery. Between day 8 to day 15, neutrophil labelling was as frequent in the core (52.2% of immunolabelled surface) as in the periphery (47.8%) of the haematoma. In the brains of patients who died more than 15 days after sICH onset, neutrophils were mostly seen in the haematoma core (76.9%).

Neutrophils within the peri-haematoma area (PHA)

Neutrophils were observed within the PHA (Figures 2C and Figures 4D,E) as early as the first 24 h (38.06 [29–46]). The MPO-labelled surface decreased by 95% in patients who died between day 4 and day 7 (2.06 [1.7–3.7], $p = 0.029$). In those who died between day 8 and day 15, we observed an 8.8-fold increase in MPO expression (17.6 [15–20], $p = 0.002$). In patients who died more than

15 days after sICH onset, the MPO-labelled surface slightly decreased (9.3 [5.9–12.7], $p = 0.173$).

Neutrophils within ipsilateral surrounding brain tissue (ISBT)

The MPO-labelled surface within ISBT (Figures 2D and Figure 4F) was low during the first 72 h (0.14 [0.13–0.15]). The MPO-labelled surface was four times higher between day 4 and day 7 (0.53 [0.48–0.62], $p = 0.025$). After day 7, the MPO-labelled surface significantly decreased (0.13 [0.12–0.30], $p = 0.007$ between day 8 and day 15 and 0.11 [0.08–0.13] after day 15). Qualitative examination showed that neutrophils were mostly perivascular but spread to the surrounding brain tissue (Figure 4F).

Evidence for the presence of NETs within the haematoma core and PHA

NETs were found in 50% ($n = 7/14$) of our study population. NETs were detected in both of the two patients' brains who died within the first 72 h, in three out of four patients who died between day 4 and day 7, and in two out of five patients who died between day 8 and day 15. No NETs were observed in any of the three patients who died after day 15 ($p = 0.016$). This temporal pattern indicated that the presence of NETs was time dependent. Among the

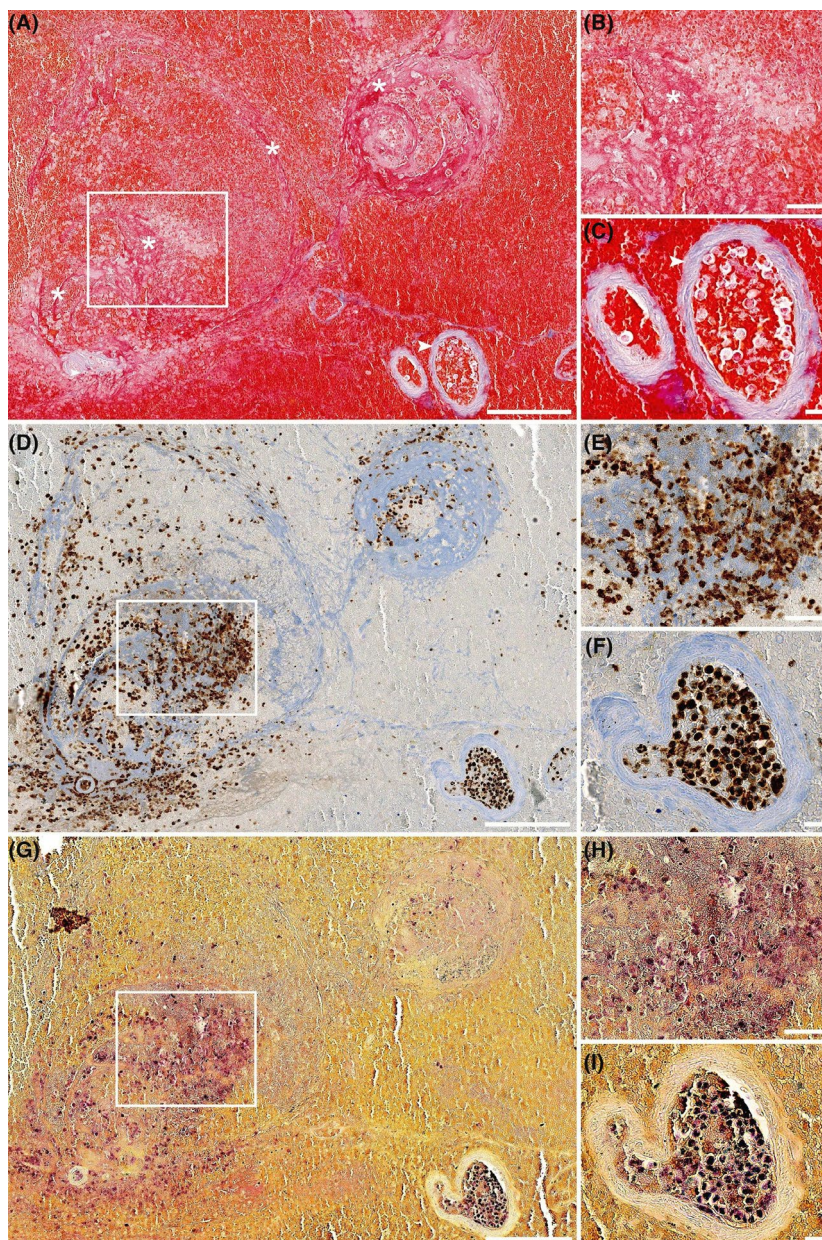


FIGURE 3 Neutrophils and neutrophil extracellular traps are located at dense fibrin fibres within intracerebral haemorrhage. Martius Scarlet Blue (MSB) staining (A, B, C), neutrophil myeloperoxidase (MPO) immunolabelling (D, E, F) and histone H3 citrulline immunolabelling (G, H, I) of adjacent slices of representative haemorrhagic areas observed in a patient who deceased after 13 days post lobar intracerebral haemorrhage (ICH). (A), (D) and (G) correspond to an overview of the examined area. (A) Fibrin fibres (pink to red) are organised into a circular pattern (asterisks), pointing to a bleeding origin at the bottom left vessel, suggestive of significant clot formation. At higher magnification (B), fibrin exhibits a dense fibrillar meshwork (asterisk), and red-stained erythrocytes show typical biconcave morphology and absence of extended haemolysis. Accumulation of non-stained cells in contact with fibrin fibres suggest the presence of leucocyte clusters. In (C), collagen (blue) delineates blood vessel walls (arrowhead) and intravascular erythrocytes and leucocytes. Abundant neutrophils in the extravasated blood are evidenced by MPO (rounded brown stain) close to light-blue fibrillar structures matching with fibrin (D), confirmed at higher magnification (E), as well as in the intravascular compartment (F). Histone H3 citrulline, corresponding to neutrophil extracellular trap (NET) formation, is disclosed both as rounded dark purple dots characteristic of intracellular staining, and as light purple smears, in areas matching with neutrophil clusters in fibrin-rich tissue sites (G), confirmed at higher magnification (H) and inside the vessel lumen (I). Scale bars = 200 μ m for A, D and G; 50 μ m for B, E and H, and 20 μ m for C, F, I

positive cases for NETs, the H3 citrulline-labelled surface within ipsilateral blocks was significantly larger than in control areas in which we did not observe any NETs ($p < 0.0001$). NETs were commonly observed in both haematoma core and PHA (Figures 3G,H

and Figures 4D,H) without significant difference between both areas ($p = 0.07$), but no NETs were observed in the ISBT (Figure 4I). The H3 citrulline-labelled surface (Figure 5A) varied with the delay after sICH onset ($p = 0.039$): NETs were observed as early as the

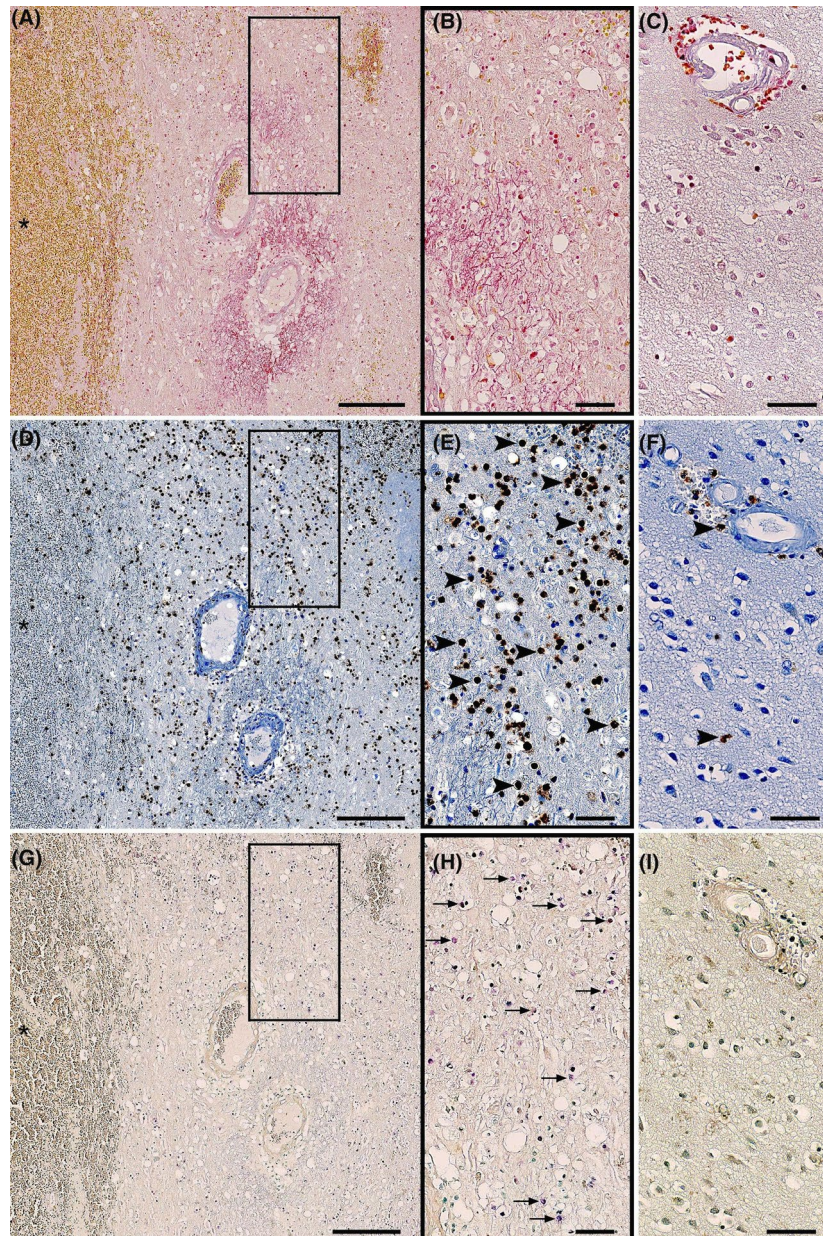


FIGURE 4 Neutrophils and neutrophil extracellular traps infiltrate the surrounding brain tissue after intracerebral haemorrhage. Martius Scarlet Blue (MSB) staining (A, B, C), neutrophil myeloperoxidase (MPO) immunolabelling (D, E, F) and histone H3 citrulline (G, H, I) immunolabelling of adjacent slices of representative peri-haematoma area (PHA) and ipsilateral surrounding brain tissue (ISBT) observed in a patient who deceased 8 days after deep intracerebral haemorrhage (ICH). (A) Blood suffusion (asterisks) at the clot border are observed through yellow-stained erythrocytes. In the PHA, tissue vacuoles and pallor suggest tissue damage and oedema, confirmed at higher magnification (B), and contrary to the ISBT area showing a homogeneous molecular layer between the soma of the more uniformly distributed brain cells (C). Abundant presence of neutrophils is evidenced in the PHA by MPO (rounded brown stain, D), confirmed at higher magnification (E, arrowheads), and contrary to the ISBT area where sparse neutrophils were found, mostly in the perivascular spaces, suggestive of recruitment from the circulation (F, arrowheads). The histone H3 citrulline of neutrophil extracellular traps (NETs) is disclosed mostly as rounded dark purple dots characteristic of intracellular signal in the PHA (G), confirmed at higher magnification (H, arrows), and contrary to the ISBT area where no NETs were found (I). Scale bars = 200 μ m for A, D and G; 50 μ m for B, C, E, F, H, and I

first 72 h (10.58 [9.7–11.5]). The labelled surface decreased by 74% between day 4 and day 7 (2.75 [2.3–3.4], $p = 0.017$). Between day 8 and day 15, we observed a 3-fold increase in NETs expression (8.61 [8.2–9.0], $p = 0.011$) that declined after 15 days ($p < 0.001$).

Qualitative examination showed smears, purple blurred signal both in haematoma core and PHA (Figure 5B,C). Interestingly, haematoma sections showed that NETs tended to agglutinate on dense fibrin fibres (Figure 3G,H).

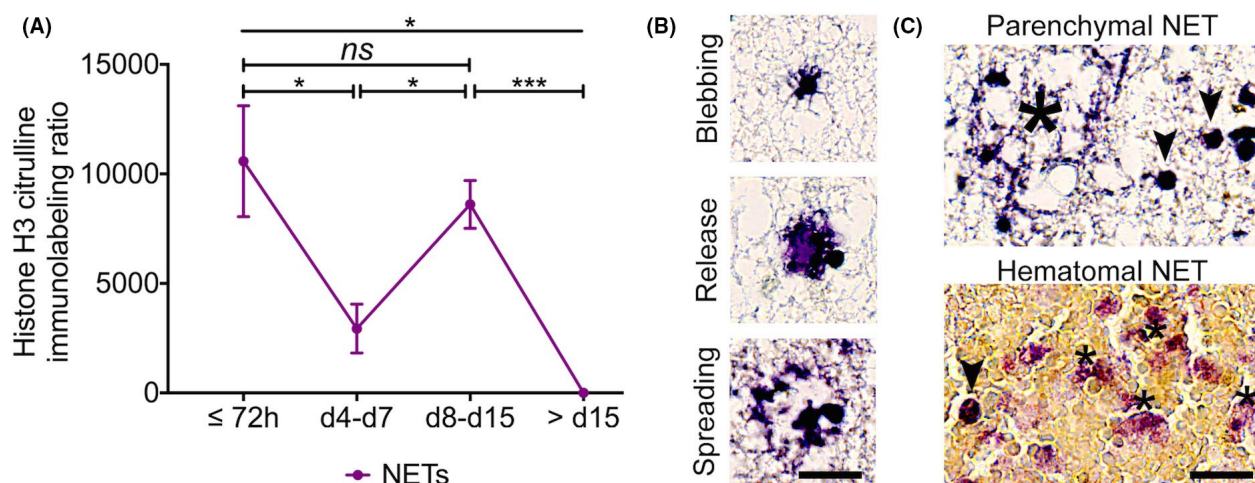


FIGURE 5 Neutrophil extracellular traps are abundant in the human brain after intracerebral haemorrhage. (A) Immunolabelling ratio ([stacking surface/whole section surface]* 10^{-3}) of citrullinated histone 3, a hallmark of neutrophil extracellular trap (NET) formation, in the post-mortem brain tissue of 14 patients who died at different time periods after intracerebral haemorrhage (before 72 h, from day 4 to day 7, from day 8 to day 15, above day 15). The curve refers to the ratios calculated in brain areas of interest where NETs were found, including the haematoma and the peri-haematoma area. Bars and symbols correspond to the median value and the width of the 95% CI. Ratios were significantly different between time points according to Kruskal-Wallis followed by a Tukey *post hoc* test (** $p \leq 0.001$, * $p \leq 0.05$; ns: not significant). (B) Representative views of different positive immunolabelling of citrullinated histone 3 (purple), suggestive of different steps of NETosis: membrane blebbing, release of decondensed chromatin to the extracellular space, and spreading of NETs in the surrounding tissue. (C) Representative views of spread NETs in the peri-haematoma area (Parenchymal NETs, large asterisk), or in the haematoma (Haematoma NETs) where multiple smears are observed (small asterisks), next to intracellular NETs (arrowheads). Scale bar = 20 μ m for (B) and 50 μ m for (C)

DISCUSSION

Four main results emerged from this post-mortem study dedicated to sICH in humans: (1) we have reported for the first time the presence of NETs after sICH in the human brain tissue, (2) NETs were released by two waves of neutrophils: during the first 72 h, and between 8 and 15 days after sICH onset, (3) neutrophils and NETs were abundant within the haematoma and the surrounding brain tissue, and (4) within the haematoma, both neutrophils and NETs were mostly seen around dense fibrin fibres.

We found NETs within the haematoma core and surrounding tissue both as extracellular smears, and more frequently as dense intracellular features. Smears refer to the first mechanism described in 2007 as the 'suicidal NETosis', where DNA/histone meshworks are cast out from the cell to trap pathogens or cell debris, leading to the death of the neutrophil.¹⁴ The intracellular feature might be just the preceding step of suicidal NETosis, or the recently reported 'vital NETosis', where the neutrophil survives since the DNA/histone meshworks are exocytosed upon activation by various stimuli including activated platelets.¹⁵

NETs are released by neutrophils, which are widely considered to be the earliest leucocytic subtype to infiltrate the haemorrhagic brain tissue. However, our knowledge on the temporal course of neutrophil infiltration in the human brain after sICH remains limited to the hyper-acute phase. Previous data obtained from 33 sICH patients showed that neutrophils infiltrate the PHA within the first 8 h, further increase in 1 day, and disappear around 72 h after sICH

onset.¹⁶ In the PHA obtained from 30 sICH patients after craniotomy, neutrophil infiltration further increased 12–24 h after sICH.¹⁷ More recently, Shtaya *et al.* observed infiltration of neutrophils within 2 days of the sICH in most cases and in all cases by 5 days post-ictus. Neutrophils were present up to 12 days.¹⁸ In line with these studies, we observed a first wave of neutrophils and NETs infiltration within the first days (≤ 72 h), but we also observed a distinct second wave occurring between day 8 and day 15. We observed perivascular neutrophils in the ISBT preceding this second wave (i.e. between day 4 and day 7), suggesting that a recruitment of neutrophils takes place at that time in the direction of PHA and the haematoma. Therefore, we hypothesise that this second wave of recruitment occurred in response to the spread of erythrocytes and possible breakdown products into the brain parenchyma, delaying the development of tissue necrosis.

During this two-wave phenomenon, we observed neutrophils and NETs both in the haematoma core and the surrounding tissue. Within the haematoma, the presence of neutrophils and NETs specifically on dense fibrin fibres was consistent with the preclinical literature. Neutrophils are known to promote clot formation through interaction with platelets, fibrin and coagulation factors.^{19–22} NETs comprise prothrombotic molecules that can trigger platelet activation and promote thrombus formation.²³ The thrombogenic potential of NETs is further supported by the experimental finding that DNase inhibits clot formation related to DNA–histone complexes.¹² In addition, the interaction between neutrophils, NETs and fibrin potentiates their respective pro-thrombotic effect.²⁴ Indeed, by

forming a DNA/plasmin/fibrin complex, the extracellular DNA of NETs pack the fibrin network densely and hinder plasmin-mediated degradation of fibrin clots, leading to clot resistance to fibrinolysis^{25,26}. Since haematoma clearance is critical, the issue of fibrinolysis resistance is of importance for sICH management. For instance, fibrinolysis resistance could explain the neutral result of the MISTIE trial since nearly 40% of patients had insufficient blood drainage despite the focal infusion of rtPA.^{2,27} Since we observed NETs in abundance within the haematoma core as early as in the first 72 h, we suggest that a pharmacomodulation of NETs activity could facilitate the fibrinolytic effect of rtPA and therefore improve the haematoma clearance. A recent experimental study in rats showed that the disintegration of NETs using DNase I could enhance fibrinolysis and promote haematoma clearance¹², opening a perspective for this treatment strategy in humans.

We observed neutrophils and NETs within the surrounding brain tissue, including the PHA and ISBT. They may contribute to the development of cerebral oedema through a deleterious pro-inflammatory process. Several experimental studies have demonstrated that neutrophils exert deleterious effects upon prolonged activation^{7,28}, including blood-brain barrier breakdown with ensuing neuronal injury, which can be directly exerted by NETs.^{11,29–32} These data were mostly observed in ischaemic stroke^{32,33}. Further experimental studies are needed to understand the influence of these NETs and neutrophils in the generation of neuroinflammation, peri-haematoma oedema growth and further necrosis after sICH. Nonetheless, we suggest that targeting neutrophils and NETs recruitment and infiltration within a delayed therapeutic window (between day 3 and day 15) might reduce secondary brain tissue damage. Several experimental treatments targeting neutrophils activation, recruitment and adhesion after ischaemic stroke have been tested but failed to prove benefit.⁷ However, our results point to a difference in the role exerted by neutrophils and NETs in the perilesional area between haemorrhagic and ischaemic strokes. Indeed, in a post-mortem study of 25 ischaemic stroke patients, Enzmann *et al.* did not find any significant neutrophil infiltration in the infarcted brain area surrounding the ischaemic core, the vast majority of neutrophils remaining close to the vasculature (intraluminal or perivascular).³⁴ Since we found neutrophils and NETs within the surrounding brain parenchyma, this therapeutic approach could be more beneficial when applied to sICH as compared to ischaemic stroke.

Finding NETs in sICH makes sense given the presence of haem-related molecules (derived from erythrolysis) has been reported to enhance the release of NETs from neutrophils.^{35,36} Recently, it has been demonstrated that haem can activate blood leukocytes and induce NET formation through an increase in intracellular reactive oxygen species (ROS).³⁷ Therefore, sICH is especially conducive to the formation of haem-induced NETs. Haem concentration following haemorrhage is mainly determined by the excess levels of cell-free haemoglobin release, involving the CD163/ haem oxygenase-1 (HO-1) pathway. CD163 is a monocyte-macrophage scavenger receptor expressed by activated microglia/macrophages. After incorporation

of the haptoglobin/haemoglobin complex, haemoglobin is broken down into Fe^{2+} and carbon oxide, and the released haem is catalysed into biliverdin by HO-1.^{38,39} Limiting NETs formation through the stimulation of HO-1 could be an interesting therapeutic strategy in ICH but the link between the CD163/HO-1 pathway, haem concentration and NETs formation has yet to be established.

Our study has some limitations. Our study population included elderly patients and sICH were associated with underlying cerebral amyloid angiopathy (CAA) in 13/14 cases. Therefore, age and underlying vessel disease may have contributed to our findings. However, patient 8 with a deep ICH showed similar histological features to lobar ICH cases, especially regarding the spatial distribution of NETs. Of note, neither neutrophil nor NETs infiltration was found in the contralateral hemispheres, suggesting that the changes observed were related to the bleeding event and not to the underlying disease. We did not perform an exhaustive examination or quantification of the entire sICH lesion. However, our assessment of neutrophil and NETs expression was performed on a substantial number of sections ($n = 2-4$) in strategic areas (ICH, PHA and ISBT). These representative samples provide a good overview of sICH and the surrounding brain damage.

Our study also has strengths. Despite the cross-sectional nature of a histopathological study, we obtained several samples at different important timepoints in the natural history of severe sICH. We used an immunohistochemistry automated staining machine and semi-automated technique to quantify immunolabelling of the sections, ensuring reproducibility of our results.

CONCLUSION

In conclusion, we showed two distinct phases of neutrophil and NETs infiltration in the human sICH brain and how many of these neutrophils entered the brain parenchyma surrounding the haematoma. Our findings provide new insights into the understanding of the mechanisms of sICH-related brain injury. Further efforts are needed to address the issue of whether this infiltration of neutrophils and NETs can lead to novel therapeutic strategies for individuals suffering from sICH.

ACKNOWLEDGMENTS

We warmly thank Marie-Hélène Gevaert, (Department of Histology, Lille), Belinda Duchène (Laboratory of Cancer Heterogeneity, Plasticity and Resistance to Therapies, UMR9020 - UMR-S 1277, Lille) and Eric Bouleaux (Univ. Lille, Inserm, CHU Lille, Institut Pasteur de Lille, U1011- EGID) for their great technical assistance in immunolabelling. We thank Dr Antonino Bongiovanni and Dr Meryem Tardivel from the Lille Bioimaging Center for their great technical assistance. Charlotte Cordonnier is a member of the Institut Universitaire de France.

CONFLICT OF INTEREST

The authors declare no conflict of interest.

AUTHORS CONTRIBUTIONS

L.P, V.B and C.C contributed to the conception and design of the study; L.P, V.B, D.C, R.P and V.D contributed to the acquisition and analysis of the data; L.P, V.B and C.C drafted the text and prepared the figures.

ETHICAL APPROVAL

All procedures performed in the study were in accordance with the ethical standards of the Lille University Regional Ethics Committee. Human brains were obtained from the Lille Neurobank (CRB/CIC1403 Biobank, BB-0033-00030, agreement DC-2008-642), which fulfils the criteria of the local laws and regulations on biological resources with donor consent, data protection, and ethical committee review.

PEER REVIEW

The peer review history for this article is available at <https://publons.com/publon/10.1111/nan.12733>.

DATA AVAILABILITY STATEMENT

All data relevant to the study are included in the article or uploaded as supplementary information. Data are available upon reasonable request.

ORCID

Laurent Puy  <https://orcid.org/0000-0002-9772-5192>

Charlotte Cordonnier  <https://orcid.org/0000-0002-5697-6892>

Vincent Bérézowski  <https://orcid.org/0000-0002-8915-5513>

REFERENCES

- van Asch CJ, Luitse MJ, Rinkel GJ, van der Tweel I, Algra A, Klijn CJ. Incidence, case fatality, and functional outcome of intracerebral haemorrhage over time, according to age, sex, and ethnic origin: a systematic review and meta-analysis. *Lancet Neurol*. 2010;9:167-176.
- Hanley DF, Thompson RE, Rosenblum M, et al. Efficacy and safety of minimally invasive surgery with thrombolysis in intracerebral haemorrhage evacuation (MISTIE III): a randomised, controlled, open-label, blinded endpoint phase 3 trial. *Lancet*. 2019;393:1021-1032.
- Cordonnier C, Demchuk A, Ziai W, Anderson CS. Intracerebral haemorrhage: current approaches to acute management. *Lancet*. 2018;392:1257-1268.
- Gong C, Hoff JT, Keep RF. Acute inflammatory reaction following experimental intracerebral hemorrhage in rat. *Brain Res*. 2000;871:57-65.
- Nguyen HX, O'Barr TJ, Anderson AJ. Polymorphonuclear leukocytes promote neurotoxicity through release of matrix metalloproteinases, reactive oxygen species, and TNF- α . *J Neurochem*. 2007;102:900-912.
- Jin R, Yang G, Li G. Inflammatory mechanisms in ischemic stroke: role of inflammatory cells. *J Leukoc Biol*. 2010;87:779-789.
- Jickling GC, Liu D, Ander BP, Stamova B, Zhan X, Sharp FR. Targeting neutrophils in ischemic stroke: translational insights from experimental studies. *J Cereb Blood Flow Metab*. 2015;35:888-901.
- Thiam HR, Wong SL, Wagner DD, Waterman CM. Cellular mechanisms of NETosis. *Annu Rev Cell Dev Biol*. 2020;36:191-218.
- Papayannopoulos V. Neutrophil extracellular traps in immunity and disease. *Nat Rev Immunol*. 2018;18:134-147.
- Ducroux C, Di Meglio L, Loyau S, et al. Thrombus neutrophil extracellular traps content impair tPA-induced thrombolysis in acute ischemic stroke. *Stroke*. 2018;49:754-757.
- Manda-Handzlik A, Demkow U. The brain entangled: the contribution of neutrophil extracellular traps to the diseases of the central nervous system. *Cells*. 2019;8(12):1477.
- Tan Q, Guo P, Zhou J, et al. Targeting neutrophil extracellular traps enhanced tPA fibrinolysis for experimental intracerebral hemorrhage. *Transl Res J Lab Clin Med*. 2019;211:139-146.
- Deramecourt V, Slade JY, Oakley AE, et al. Staging and natural history of cerebrovascular pathology in dementia. *Neurology*. 2012;78:1043-1050.
- Fuchs TA, Abed U, Goosmann C, et al. Novel cell death program leads to neutrophil extracellular traps. *J Cell Biol*. 2007;176:231-241.
- Jorch SK, Kubes P. An emerging role for neutrophil extracellular traps in noninfectious disease. *Nat Med*. 2017;23:279-287.
- Mackenzie JM, Clayton JA. Early cellular events in the penumbra of human spontaneous intracerebral hemorrhage. *J Stroke Cerebrovasc Dis*. 1999;8:1-8.
- Guo F, Li X, Chen L, et al. Study of relationship between inflammatory response and apoptosis in perihematoma region in patients with intracerebral hemorrhage. *Zhongguo Wei Zhong Bing Ji Jiu Yi Xue*. 2006;18:290-293.
- Shtaya A, Bridges LR, Esiri MM, et al. Rapid neuroinflammatory changes in human acute intracerebral hemorrhage. *Ann Clin Transl Neurol*. 2019;6:1465-1479.
- Ruff CT, Giugliano RP, Braunwald E, et al. Comparison of the efficacy and safety of new oral anticoagulants with warfarin in patients with atrial fibrillation: a meta-analysis of randomised trials. *Lancet*. 2014;383:955-962.
- Pfeiler S, Stark K, Massberg S, Engelmann B. Propagation of thrombosis by neutrophils and extracellular nucleosome networks. *Haematologica*. 2017;102:206-213.
- Darbousset R, Thomas GM, Mezouar S, et al. Tissue factor-positive neutrophils bind to injured endothelial wall and initiate thrombus formation. *Blood*. 2012;120:2133-2143.
- Goel MS, Diamond SL. Neutrophil enhancement of fibrin deposition under flow through platelet-dependent and -independent mechanisms. *Arterioscler Thromb Vasc Biol*. 2001;21:2093-2098.
- Semeraro F, Ammolio CT, Morrissey JH, et al. Extracellular histones promote thrombin generation through platelet-dependent mechanisms: involvement of platelet TLR2 and TLR4. *Blood*. 2011;118:1952-1961.
- Varju I, Kolev K. Networks that stop the flow: A fresh look at fibrin and neutrophil extracellular traps. *Thromb Res*. 2019;182:1-11.
- Longstaff C, Varju I, Sotonyi P, et al. Mechanical stability and fibrinolytic resistance of clots containing fibrin, DNA, and histones. *J Biol Chem*. 2013;288:6946-6956.
- Staessens S, Denorme F, Francois O, et al. Structural analysis of ischemic stroke thrombi: histological indications for therapy resistance. *Haematologica*. 2020;105:498-507.
- Hanley DF, Lane K, McBee N, et al. Thrombolytic removal of intraventricular haemorrhage in treatment of severe stroke: results of the randomised, multicentre, multicentre, placebo-controlled CLEAR III trial. *Lancet*. 2017;389:603-611.
- Segel GB, Halterman MW, Lichtman MA. The paradox of the neutrophil's role in tissue injury. *J Leukoc Biol*. 2011;89:359-372.
- Kolaczowska E, Kubes P. Neutrophil recruitment and function in health and inflammation. *Nat Rev Immunol*. 2013;13:159-175.
- Matsuo Y, Onodera H, Shiga Y, et al. Correlation between myeloperoxidase-quantified neutrophil accumulation and ischemic brain injury in the rat. Effects of neutrophil depletion. *Stroke*. 1994;25:1469-1475.
- Weston RM, Jones NM, Jarrott B, Callaway JK. Inflammatory cell infiltration after endothelin-1-induced cerebral ischemia:

- histochemical and myeloperoxidase correlation with temporal changes in brain injury. *J Cereb Blood Flow Metab.* 2007;27:100-114.
32. Allen C, Thornton P, Denes A, et al. Neutrophil cerebrovascular transmigration triggers rapid neurotoxicity through release of proteases associated with decondensed DNA. *J Immunol.* 2012;189:381-392.
 33. Perez-de-Puig I, Miro-Mur F, Ferrer-Ferrer M, et al. Neutrophil recruitment to the brain in mouse and human ischemic stroke. *Acta Neuropathol.* 2015;129:239-257.
 34. Enzmann G, Mysiorek C, Gorina R, et al. The neurovascular unit as a selective barrier to polymorphonuclear granulocyte (PMN) infiltration into the brain after ischemic injury. *Acta Neuropathol.* 2013;125:395-412.
 35. Kono M, Saigo K, Takagi Y, et al. Heme-related molecules induce rapid production of neutrophil extracellular traps. *Transfusion.* 2014;54:2811-2819.
 36. Porto BN, Alves LS, Fernandez P, et al. Heme induces neutrophil migration and reactive oxygen species generation through signaling pathways characteristic of chemotactic receptors. *J Biol Chem.* 2007;282:24430-24436.
 37. Chen G, Zhang D, Fuchs TA, Manwani D, Wagner DD, Frenette PS. Heme-induced neutrophil extracellular traps contribute to the pathogenesis of sickle cell disease. *Blood.* 2014;123:3818-3827.
 38. Cao S, Zheng M, Hua Y, Chen G, Keep RF, Xi G. Hematoma changes during clot resolution after experimental intracerebral hemorrhage. *Stroke.* 2016;47:1626-1631.
 39. Li Q-Q, Li L-J, Wang X-Y, Sun Y-Y, Wu J. Research progress in understanding the relationship between heme oxygenase-1 and intracerebral hemorrhage. *Front Neurol.* 2018;9:682.

How to cite this article: Puy L, Corseaux D, Perbet R, Deramecourt V, Cordonnier C, Bérézowski V. Neutrophil extracellular traps (NETs) infiltrate haematoma and surrounding brain tissue after intracerebral haemorrhage: A post-mortem study. *Neuropathol Appl Neurobiol.* 2021;47:867–877. <https://doi.org/10.1111/nan.12733>